APPLIED SCIENCES AND ENGINEERING

Small-scale universality in the spectral structure of transitional pipe flows

Rory T. Cerbus[1], Chien-chia Liu[1], Gustavo Gioia[2], Pinaki Chakraborty[1]*

Turbulent flows are not only everywhere, but every turbulent flow is the same at small scales. The extraordinary simplification engendered by this "small-scale universality" is a hallmark of turbulence theory. However, on the basis of the restrictive assumptions invoked by A. N. Kolmogorov to demonstrate this universality, it is widely thought that only idealized turbulent flows conform to this framework. Using experiments and simulations that span a wide range of Reynolds number, we show that small-scale universality governs the spectral structure of a class of flows with no apparent ties to the idealized flows: transitional pipe flows. Our results not only extend the universality of Kolmogorov's framework beyond expectation but also establish an unexpected link between transitional pipe flows and Kolmogorovian turbulence.

INTRODUCTION

Kolmogorovian turbulence at very large Reynolds numbers

Every turbulent flow looks different. Yet, many will look the same when placed under a magnifying glass; the statistics of the small scales are universal, irrespective of the particular flow. This is the key insight of Kolmogorov's phenomenological theory of turbulence (1–3). The theory is built on Richardson's imagery of an "energy cascade" (4): The energy progressively cascades from large scales to smaller scales to even smaller scales and so forth, until it is dissipated viscously at the smallest scales.

Kolmogorov crystallized this imagery into quantitative predictions (1–3). At each step of the cascade, the nonlinear interactions that mediate the scale-to-scale transfer of energy also cause a progressive loss of sensitivity to the large-scale attributes of the flow. The larger the Reynolds number, Re, the broader the separation between large and small scales and, consequently, the lesser the influence of the large scales on the distant small scales. Considering turbulent flows at "very large Re" (1) and in regions far from boundaries, Kolmogorov posited that whereas the large scales can be inhomogeneous, anisotropic, and unsteady, the statistics of small scales turn homogeneous, isotropic, and steady. Kolmogorov called this property of small scales "local isotropy" (1).

For this domain of small scales, Kolmogorov made the bold hypothesis—the "first similarity hypothesis"—that their statistics depend only on the kinematic viscosity, ν; the energy dissipation rate per unit mass, ε; and the wave number, k. This hypothesis, in the domain $k \gg L^{-1}$ (where L is a large scale, e.g., pipe diameter), leads to a universal function for the energy spectrum, $E(k)$, which embodies the spectral structure of the velocity fluctuations; specifically

$$E(k) \propto \frac{\nu^2}{\eta} F(\eta k) \tag{1}$$

where $\eta \equiv (\nu^3/\varepsilon)^{1/4}$ is the viscous dissipation scale (also known as the Kolmogorov scale) and $F(\eta k)$ is a universal function—a mathematical signature of small-scale universality (1). At this juncture, we

also mention Kolmogorov's "second similarity hypothesis," according to which, in a subdomain of small-scale universality—the "inertial range," $L^{-1} \ll k \ll \eta^{-1}$—$E(k) \propto \varepsilon^{2/3} k^{-5/3}$ [i.e., $F(\eta k) \propto (\eta k)^{-5/3}$], the "5/3 law." Notwithstanding its prestige, we emphasize that it is conformity to the universal $F(\eta k)$ that signals small-scale universality, regardless of the specific functional form of F. In discussing small-scale universality, we limit our attention to $E(k)$, which is a second-order statistical measure, although Kolmogorov's theory also extends to higher-order statistics.

To test Kolmogorov's predictions, field observations, experiments, and simulations have naturally reached toward flows with ever larger Re (5–7). Furthermore, these studies have often sought to draw as close as possible to ideal conditions, meaning homogeneity, isotropy, and steadiness in the large scales as well. The evidence in all cases is overwhelmingly in favor of Kolmogorov's predictions, and although there are well-known deviations (anomalous scaling) for higher-order statistics (8), his original framework remains the most lucid and empirically tested description of turbulence at very large Re.

Unexpectedly, recent studies have shown that Kolmogorov's theory prevails even at moderate values of Re (9, 10). Evidently, the realm of Kolmogorovian turbulence is much broader than previously anticipated. In this study, we put the limits of this realm to an extreme test by considering flows that are far removed from any turbulent flow studied heretofore. They are relatively low Re, inhomogeneous (segmented along the flow direction and fully circumscribed by walls), and unsteady (the segmented regions change with time) transitional pipe flows (11).

Transition to turbulence in pipe flows

Pipe flows are linearly stable (12–14). But for finite-amplitude perturbations, the flow can remain laminar up to arbitrarily large Re (by definition, Re $\equiv UD/\nu$, where U is the mean flow velocity and D is the pipe diameter). For Re $\lesssim 1600$, irrespective of the perturbations, the flow is laminar throughout the pipe. At higher Re, the existence of laminar flow is predicated on the perturbations being small. For perturbations of finite amplitude above a critical threshold [which decreases with increase in Re (12)], other flow states become manifest. At the onset of transition, laminar flow becomes axially inhomogeneous, with plugs of laminar flow alternating with "flashes" of eddying flow (11–13). Flashes come in two states. For $1600 \lesssim$ Re $\lesssim 2250$, flashes take the form of arrowhead-shaped, discrete lumps
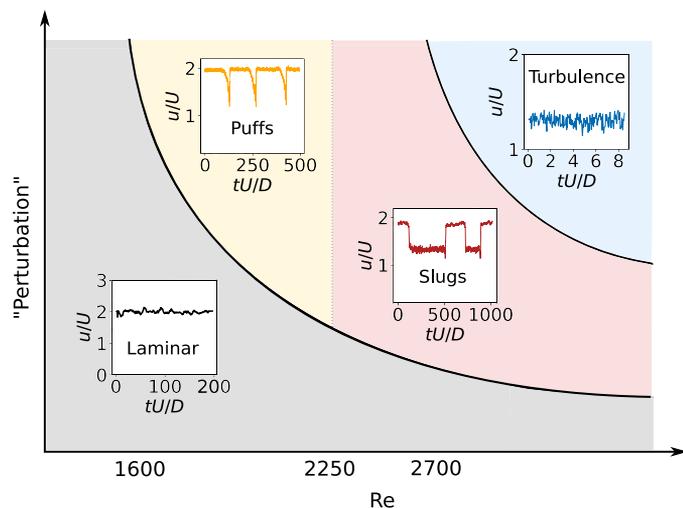
[1]Fluid Mechanics Unit, Okinawa Institute of Science and Technology Graduate University, Onna-son, Okinawa 904-0495, Japan. [2]Continuum Physics Unit, Okinawa Institute of Science and Technology Graduate University, Onna-son, Okinawa 904-0495, Japan.
*Corresponding author. Email: pinaki@oist.jp

($\sim$20D long) of chaotic flow called "puffs." Laminar flow continually invades a puff from the tail, turns into fluctuating flow as it sweeps its length, and returns to laminar flow as it exits from the arrow-shaped head. As they flow downstream, puffs can maintain a fixed size or spontaneously split to form new puffs or spontaneously fade away into the surrounding laminar flow. At Re $\approx$ 2250, a new breed of flashes emerges. Called "slugs," they expand inexorably as they flow downstream. For Re $\gtrsim$ 2700, the flow state depends on whether the finite-amplitude perturbation is applied briefly or continuously. For the former, slugs persist; for the latter, the flow turns to fully developed turbulence throughout the pipe. In Fig. 1, we illustrate this sequence of flow states.

Study

We focus on flash flow or flow inside flashes. For reference, we note that even for fully turbulent pipe flows, small-scale universality appears to have been tested (and found to hold) only for Re $\geq$ 24,000 (15); whether small-scale universality holds for Re < 24,000 is not known. Now, flashes span values of Re that are an order of magnitude lower. They appear, on the basis of their macroscopic features, qualitative as well as quantitative, clearly distinct from turbulence (16, 17). Above, we have discussed a few qualitative features, e.g., the arrowhead shape of puffs. Complementing the distinctions highlighted by the qualitative features, quantitative features draw attention to the role of Re. For example, the lifetime statistics for puffs splitting and the lifetime statistics for puffs fading away markedly change depending on whether the Re is above or below a critical Re (12, 14); the speeds of the front and back interfaces of the expanding slugs vary systematically with Re (16, 18). To wit, given the low Re and marked differences with turbulent flows, a priori, it appears unlikely that flash flows could partake in the signature universality of Kolmogorovian turbulence.
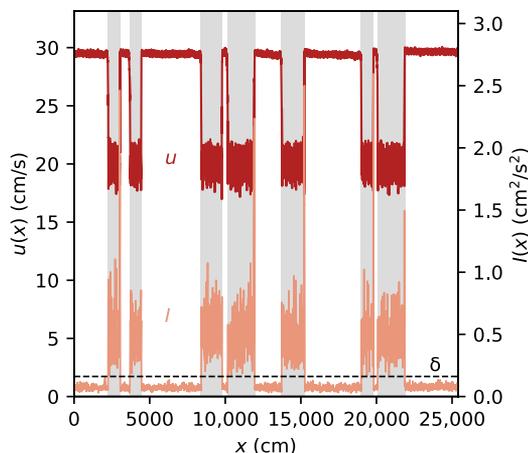
We examine flash flows with a combination of experiments and direct numerical simulations (DNS). For the experiments, we use a 20-m-long, smooth, cylindrical glass pipe of D = 2.5 cm $\pm$ 10 μm with water as the working fluid. For the DNS, we use the open-source, hybrid-spectral code Openpipeflow (19). Details about the experiments and DNS can be found in (20).

We first focus on the flow along the centerline of the pipe (we consider off-centerline flow later). For the experiments, we measure a time series of the axial velocity and radial velocity, $u(t)$ and $v(t)$, respectively, where t is time, using a laser Doppler velocimeter (LDV) (see Materials and Methods). We invoke Taylor's frozen turbulence hypothesis to transform the velocity time series to the velocity spatial series (see the Supplementary Materials). (For flash flows, it is not obvious a priori that Taylor's hypothesis is valid. We discuss this issue in detail in the Supplementary Materials; here, it suffices to note that Taylor's hypothesis holds for flash flows.) For the DNS, we directly obtain the velocity spatial series. Note that for transitional flows, the velocity series from experiments and DNS include flashes and laminar plugs. We disentangle the flashes using an indicator function (see Fig. 2). Having identified the regions of flash flow, we are ready to proceed.

RESULTS

Local isotropy

In accord with the sequence of arguments in Kolmogorov's analysis (1), before considering small-scale universality, we first test for local isotropy. To that end, we study a scale-by-scale measure of isotropy: $E_{xr}(k)$, the cospectrum of u and v (21), whose dimensionless form, known as the spectral coherency (22), is defined as $H_{xr}(k) \equiv |E_{xr}(k)|^2 / (E_{xx}(k)E_{rr}(k))$, where $E_{xx}(k)$ and $E_{rr}(k)$ are the (one-dimensional) energy spectra of the axial and radial components, respectively, and k is the

Fig. 1. A schematic "state diagram" for pipe flows. The abscissa is Re, and the ordinate is a qualitative measure of the perturbation. For laminar flow, puffs, and slugs (at Re $\lesssim$ 2700), the measure of the perturbation is primarily its amplitude. When the amplitude is below a critical value (which decreases with increase in Re), the flow stays laminar; when the amplitude exceeds this critical value, the other flow states are triggered. For slugs (at Re $\gtrsim$ 2700) and turbulence, the measure of the perturbation, in addition to its amplitude exceeding the critical value, is whether the perturbation is applied briefly (which yields slugs) or continuously (which yields turbulence). Corresponding to each flow state, we show representative experimental time series of the axial velocity at the pipe centerline.

Fig. 2. An illustrative example of identifying slugs using LDV data. To identify the regions of slug flow (or, in general, flash flow), we define an indicator function $I(x)$, where x is the axial distance, using squared off-axis velocity components (see the Supplementary Materials). Because the magnitude of the off-axis velocities are small for laminar plugs but substantial for flashes, the flashes can be robustly identified by putting a threshold on $I(x)$. In the example here, we show simultaneous spatial series of the axial velocity, $u(x)$, and the indicator function, $I(x)$. The slugs correspond to $I(x) \geq \delta$ (marked by gray bars), where the threshold δ (dashed line) is set as 3 SDs above the mean laminar value of $I(x)$ (20, 27).

axial wave number. (We compute the energy spectra and the co-spectrum using the velocity spatial series attendant to flash flows and turbulent flows; see the Supplementary Materials.) This measure is built on the idea that for the scales where the velocity components become statistically independent, there is no preferred direction in the attendant flow. In choosing this measure, we follow the well-known exposition on local isotropy by Saddoughi and Veeravalli (22), who concluded that $E_{xr}(k)$ is "the most sensitive indicator of local isotropy." Specifically, $H_{xr}(k) \ll 1$ at large k signals local isotropy.

In Fig. 3A, we show $|E_{xr}(k)|$, along with the corresponding $E_{xx}(k)$ and $E_{rr}(k)$, for a representative puff flow, slug flow, and turbulent flow. In Fig. 3B, we show the corresponding $H_{xr}(k)$. For all flows, across the whole domain of k, $|E_{xr}(k)|$ assumes values an order of magnitude lower than the corresponding $E_{xx}(k)$ and $E_{rr}(k)$. This comparison is rendered quantitative by $H_{xr}(k)$; we find that $H_{xr}(k) \ll 1$ for all k. At the pipe centerline, the flows not only are in good accord with local isotropy but also manifest isotropy at the large scales.

Small-scale universality
Having verified local isotropy, we test for small-scale universality, as embodied by Eq. 1. In Fig. 4A, we show $E(k)$ for several representative puff flows, slug flows, and turbulent flows from our experiments and DNS, along with a few high-Re $E(k)$ from the Princeton superpipe experiment (15, 23). [In our analysis of $E(k)$, we restrict our attention to $E_{xx}(k)$. Focusing on this most commonly studied component of the energy spectrum allows us to compare our results with those from other studies at very large Re. Hereafter, we refer to $E_{xx}(k)$ simply as $E(k)$.] Each $E(k)$ is a distinct curve whose shape depends on the particular flow realization (specifically, on the values of U, D, and ν). Spanning a range of Re, from 1600 to 512,000, these spectra differ widely and betray no sign of universality. In Fig. 4B, we rescale these spectra as per Eq. 1: The abscissa is rescaled as ηk, and the ordinate is rescaled as $\eta E(k)/\nu^2$. (See the Supplementary Materials for details of computing η.) For all flows—whether they be high-Re turbulent flows, moderate-Re turbulent flows, slug flows, or even puff flows—the rescaled spectra at high ηk collapse onto a common

curve, which we identify as the universal function $F(\eta k)$ of Eq. 1. In other words, despite appearing to constitute disparate flow states, puffs, slugs, and turbulence all conform to the framework of small-scale universality.

Besides the collapse onto the universal $F(\eta k)$, another salient feature of Fig. 4B is that the rescaled spectra peel off from $F(\eta k)$ at a value of ηk, say ηk^*, that lessens monotonically with increase in Re. We discuss this feature next. As noted earlier, small-scale universality pertains to $k \gg D^{-1}$. Identifying its lower limit as $k^* \propto D^{-1}$, we get $\eta k^* \propto \eta/D$. To understand the Re dependence of ηk^*, we now turn our attention to η/D.

### Scaling of the Kolmogorov scale
At the bottom of the energy cascade, the smallest scales (of size $\sim\eta$) viscously dissipate energy (per unit mass) at a rate equal to ε. A central concept of the Kolmogorovian framework is that the value of ε is dynamically set by the largest scales (of size $\sim D$ and velocity $\sim U$). When the largest scales are unaffected by viscosity, so is ε [the independence of ε from viscosity is known as the "dissipation anomaly" (2, 24)]. Dimensional considerations yield $\varepsilon \propto U^3/D$ (2, 24); thus, U^3/D is the only large-scale attribute that the cascade conveys to the small scales. Substituting $\varepsilon \propto U^3/D$ in the definition $\eta \equiv (\nu^3/\varepsilon)^{1/4}$, we get the Kolmogorovian scaling

$$\frac{\eta}{D} \propto \mathrm{Re}^{-3/4} \qquad (2)$$

which links the microscopic length scale of the fluctuating flow, η, with two macroscopic parameters of the mean flow, D and Re.

Note that unlike the 5/3 law, Eqs. 1 and 2 are not predicated on having a broad inertial range, which necessitates a small ratio η/D, which, in turn, necessitates a particularly large value of Re (see Eq. 2). For pipe flows, the 5/3 law becomes clearly apparent (23) only for Re > 80,000, well above the values of Re at which flashes have been observed. By contrast, Eqs. 1 and 2 can hold, in principle, at the values of Re of our experiments (note, however, that whereas the 5/3 law can be tested by using a single flow realization at very large
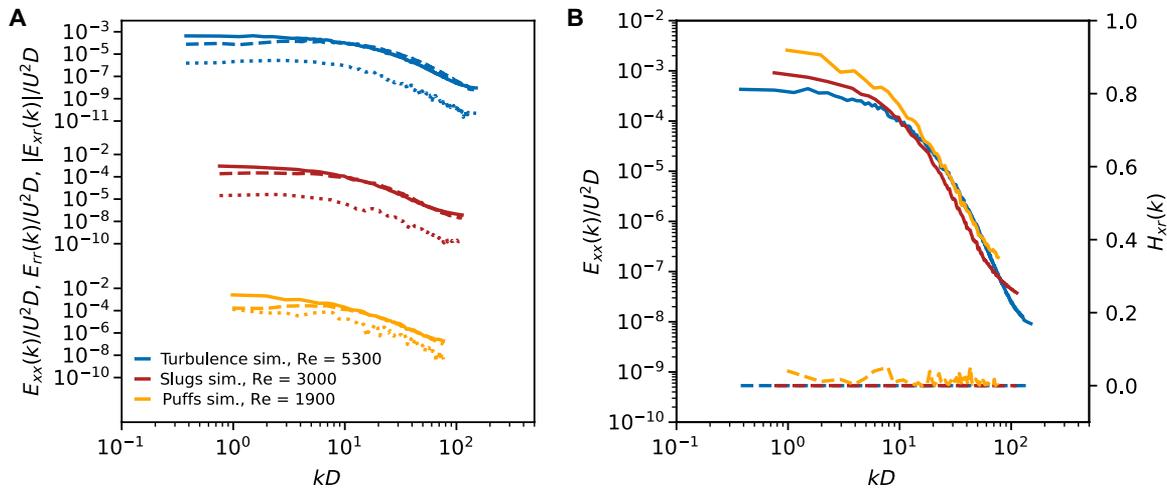
Fig. 3. Testing local isotropy for centerline flow. (**A**) Plots of $|E_{xr}(k)|U^2/D$ versus kD (dotted lines), $E_{xx}(k)U^2/D$ versus kD (solid lines), and $E_{rr}(k)U^2/D$ vs. kD (dashed lines) for a representative puff flow, slug flow, and turbulent flow from our DNS. Note the ordinate axis: for ease of comparison, we show the set of spectra plots for each flow separately. (**B**) Plots of $H_{xr}(k)$ versus kD (dashed lines) corresponding to the flows in (A). For reference, we replot the $E_{xx}(k)$ (solid lines). Note that $H_{xr}(k) \ll 1$ for all k.
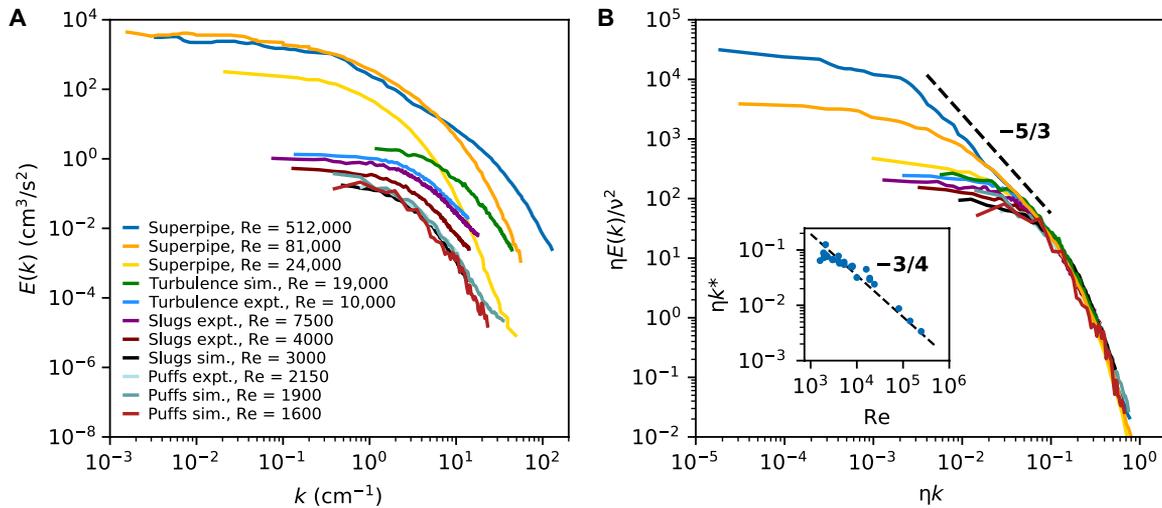
Fig. 4. Testing small-scale universality (Eq. 1) for centerline flow. (**A**) Plots of spectra, $E(k)$ versus k, for several representative puff flows, slug flows, and turbulent flows from our experiments and DNS; we also show a few high-Re turbulent flows from the superpipe experiment (15, 23). (**B**) Plots of rescaled spectra, $\eta E(k)/\nu^2$ versus ηk, corresponding to the flows in (A). Irrespective of the type of flow, the rescaled spectra at high ηk collapse onto $F(\eta k)$, in good keeping with small-scale universality (Eq. 1) [we take the $\eta k \gtrsim 10^{-2}$ region of the rescaled spectrum from superpipe flow at Re = 512,000 as a proxy for $F(\eta k)$]. At Re $\gtrsim$ 80,000, the rescaled spectra conform not only to small-scale universality but also to the 5/3 law. Inset: The scaling of data points (ηk^*, Re) is also in accord with the Kolmogorovian framework. We compute k^* by putting a threshold on the deviation of the rescaled spectra from $F(\eta k)$. The dashed line—the least-squares fit to the prediction $\eta k^* \propto$ Re$^{-3/4}$—represents $\eta k^* = 34.7$Re$^{-3/4}$, which, from the fit of Fig. 5, yields $k^* \approx 5D^{-1}$.
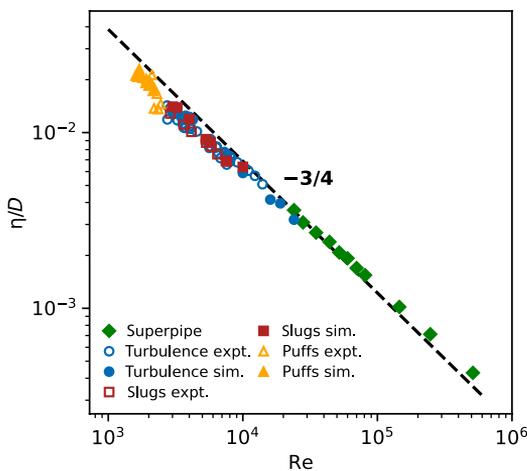
Fig. 5. Scaling of the Kolmogorov scale. Data points (η/D, Re) for centerline flow from all our experiments, DNS, and several high-Re superpipe experiments (15). The data are in good keeping with Eq. 2, irrespective of the type of flow. The dashed line—the least-squares fit to Eq. 2—represents $\eta/D = 6.88$Re$^{-3/4}$. The ratio η/D is a measure of the separation between the large and small scales; the separation broadens with an increase in Re. Note that even for puff flow at Re = 1600, $\eta/D \approx 0.027 \ll 1$, signaling a broad separation of scales.

Re, a test of Eqs. 1 and 2 requires many flow realizations that span a broad range of Re). In the previous section, we showed that Eq. 1 holds for our experiments; next, we turn to testing Eq. 2.

In Fig. 5, we test Eq. 2 using data points corresponding to puff flows, slug flows, and turbulent flows from all our experiments and DNS, along with several data points corresponding to high-Re turbulent flows from the Princeton superpipe experiment (15, 23). Irrespective of the type of flow or the value of Re (which spans about two decades), the data points conform to the Kolmogorovian scaling of Eq. 2 [in all cases that we studied, the Taylor microscale Reynolds

number Re$_\lambda \gtrsim$ 60, for which we find that Eq. 2 holds, in accord with previous studies that find the dissipation anomaly requires Re$_\lambda \gtrsim$ 20 to 50 (9, 25)]. Returning to ηk^*, using Eq. 2, we predict that $\eta k^* \propto \eta/D \propto$ Re$^{-3/4}$. In the inset of Fig. 4B, we verify this prediction.

Off-centerline flow

Thus far, we have restricted our attention to the flow along the pipe centerline. While our finding that flash flows conform to the Kolmogorovian framework, even if this holds only at the centerline, is unexpected, it is natural to ask whether this framework also extends away from the centerline. Two challenges become immediately apparent. First, the pipe geometry makes the flow progressively more inhomogeneous as the wall is approached. Second, whereas the mean shear at the centerline is zero, it monotonically increases away from the centerline, and because mean shear engenders anisotropy, the increased mean shear makes the flow progressively more anisotropic as the wall is approached. Consequently, whether off-centerline flash flow, or even turbulent flow, will exhibit local isotropy and small-scale universality is unclear. We now turn our attention to these considerations. (Because our experimental measurements are restricted to the centerline, here, we use only our DNS data.)

To test for local isotropy, in Fig. 6A, we show $H_{xr}(k)$ for a representative puff flow, slug flow, and turbulent flow at three wall-normal positions, y, that span $0.05 \leq y/D \leq 0.5$. In each flow and for all the positions, $H_{xr}(k) \ll 1$ at high ηk, signaling local isotropy. By contrast, at low ηk, for positions away from the centerline, $H_{xr}(k) \ll 1$ no longer holds, signaling that the large scales are anisotropic.

Having verified local isotropy, we test for small-scale universality (Eq. 1). In Fig. 6B, we show the rescaled spectra, $\eta E(k)/\nu^2$ versus ηk, for several representative puff flows, slug flows, and turbulent flows, spanning the wall-normal positions $0.05 \leq y/D \leq 0.5$. For all flows, regardless of the type and the value of Re, and over the whole span of positions, the rescaled spectra at high ηk collapse onto the same
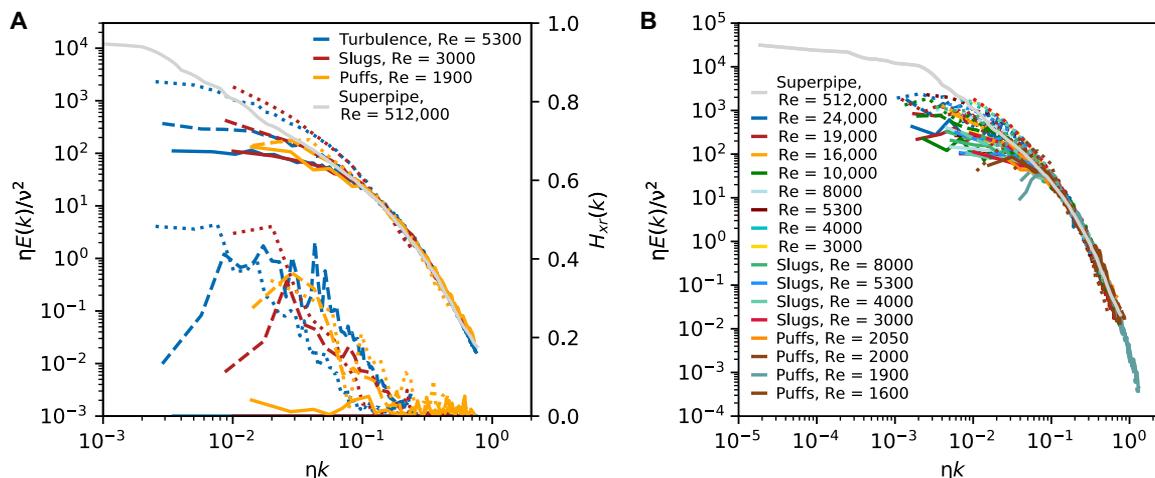
Fig. 6. Testing local isotropy and small-scale universality for off-centerline flow. (**A**) Plots of $H_{xr}(k)$ versus ηk and $\eta E(k)/\nu^2$ versus ηk for a representative puff flow, slug flow, and turbulent flow from our DNS. For each flow, we plot three wall-normal positions: $y/D = 0.5$ (solid lines), $y/D = 0.25$ (dashed lines), and $y/D = 0.05$ (dotted lines). At high ηk, local isotropy holds [$H_{xr}(k) \ll 1$], and in this domain, the rescaled spectra collapse onto a common curve. (**B**) Plots of $\eta E(k)/\nu^2$ versus ηk for several representative puff flows, slug flows, and turbulent flows from our DNS; the wall-normal positions are the same as in (A) (in the legend, the Re values without an associated flow type refer to turbulent flows). As in Fig. 4B, as a proxy for $F(\eta k)$, here, in both panels, we show the centerline spectrum from superpipe flow at Re = 512,000 (*23*). For all flows, from Re = 1600 puff flow to Re > 500,000 superpipe flow, and spanning the wall-normal positions $0.05 \leq y/D \leq 0.5$, the rescaled spectra at high ηk collapse onto $F(\eta k)$, a signature of small-scale universality.

universal function $F(\eta k)$ as we noted in Fig. 4B. The framework of small-scale universality truly has a broad purchase (for additional discussion, see the Supplementary Materials).

DISCUSSION

In summary, we have shown that the spectral structure of the small-scale fluctuations in flash flows, like those in conventional turbulent flows, is governed by Kolmogorov's phenomenological theory of turbulence, with the implication that flash flows, aside from being restricted to relatively low Re, are statistically indistinguishable from conventional turbulent flows. This finding harks back to the early studies on transitional flows and fully turbulent flows, which treated them as part of the same tapestry before later developments sundered them into divergent fields (*26*). Our findings notably broaden the scope of Kolmogorovian turbulence, extending its realm much beyond the restricted domain of idealized flows at very large Re, suggesting that the theory may truly be universal.

Our findings also provide a critical missing piece of empirical evidence in support of recent studies that seek the universality class of transitional pipe flows. In a number of experimental and computational studies (*27–29*) published in 2016, compelling evidence has been adduced in support of a 30-year-old conjecture by Pomeau (*30*) to the effect that the subcritical transition in pipe flows and other shear flows belongs to the directed-percolation universality class of nonequilibrium phase transitions. Yet, in a comment on those studies (*31*), Pomeau cautioned that "the arrowhead patterns observed in early experiments [on boundary layers] are sufficiently regular to denote a bifurcation to a turbulence-free state." (Recall that puffs, too, are shaped like arrowheads.) That is to say, if flashes were nonturbulent, then they could hardly be the agents of a transition to turbulence, and the experimental and computational evidence of directed percolation would be severed from the turbulent regime. Our findings show that flash flow is but turbulent flow; thus, flashes endow the transitional regime with the requisite link to turbulence.

We submit that the tools of high-Re turbulence can be brought to bear upon flashes and that new insights into the transition to turbulence may be gained by approaching the transition from above, from higher to lower Re, complementing the usual approach from below. For example, invoking the spectral link (*32, 33*) and using Eq. 2, we can predict that the fluid friction corresponding to the flashes obeys the Blasius scaling, as indeed has been recently verified using experiments and simulations (*20*). With elegant simplicity, Kolmogorov's phenomenal insight, from 1941, into the mechanics of complex turbulent flows at very large Re continues to also illuminate problems far removed from its original scope.

MATERIALS AND METHODS
Velocity measurements
We used an LDV (Dantec FiberFlow) to measure the time series $u(t)$ and $v(t)$. The LDV was stationed at a distance of $465D$ (1162.5 cm) from the entrance of the pipe [see the Supplementary Materials in (*20*) for details of the experimental setup]. At this location, the pipe was housed inside a rectangular acrylic encasement filled with water; this was to reduce optical distortion (see fig. S1) [this design is similar to that used in (*34*)]. Despite the optical encasement, there was still a small correction to $v(t)$, which, via ray tracing (*35*), we estimated to be $v_{real}(t) \approx 1.026 v_{measured}(t)$. To conduct LDV measurements, we seeded the water in the pipe with 10-μm-diameter, silver-coated, density-matched particles. The typical data rate was >300 Hz, and the typical length of a time series was ≈1000 s.

SUPPLEMENTARY MATERIALS
Supplementary material for this article is available at http://advances.sciencemag.org/cgi/content/full/6/4/eaaw6256/DC1
Supplementary Text
Fig. S1. Velocity measurements.
Fig. S2. Test of Taylor's hypothesis.
Fig. S3. Effect of the choice of the value of δ on the value of η.
Fig. S4. Effect of detrending in puff flows.

Fig. S5. Ratio tests for isotropy.
Fig. S6. Testing the validity of the isotropic formula in computing η for centerline flow.
Fig. S7. Dissipation spectrum.
Fig. S8. η/*D* versus Re.
Fig. S9. Effect of mean shear on small scales.
References (*36–43*)

REFERENCES AND NOTES

1. A. N. Kolmogorov, The local structure of turbulence in incompressible viscous fluid for very large Reynolds' numbers. *Dokl. Akad. Nauk SSSR* **30**, 301–305 (1941).
2. G. K. Batchelor, *The Theory of Homogeneous Turbulence* (Cambridge Univ. Press, 1953).
3. U. Frisch, *Turbulence: The Legacy of A. N. Kolmogorov* (Cambridge Univ. Press, 1995).
4. L. F. Richardson, *Weather Prediction by Numerical Process* (Cambridge Univ. Press, 1922).
5. H. L. Grant, R. W. Stewart, A. Moilliet, Turbulence spectra from a tidal channel. *J. Fluid Mech.* **12**, 241–268 (1962).
6. A. S. Monin, A. M. Yaglom, *Statistical Fluid Mechanics* (Dover, 2007), vol. 2.
7. T. Ishihara, T. Gotoh, Y. Kaneda, Study of high-Reynolds number isotropic turbulence by direct numerical simulation. *Annu. Rev. Fluid Mech.* **41**, 165–180 (2009).
8. G. Falkovich, K. R. Sreenivasan, Lessons from hydrodynamic turbulence. *Phys. Today* **59**, 43 (2006).
9. R. A. Antonia, L. Djenidi, L. Danaila, Collapse of the turbulent dissipative range on Kolmogorov scales. *Phys. Fluids* **26**, 045105 (2014).
10. J. Schumacher, J. D. Scheel, D. Krasnov, D. A. Donzis, V. Yakhot, K. R. Sreenivasan, Small-scale universality in fluid turbulence. *Proc. Natl. Acad. Sci. U.S.A.* **111**, 10961–10965 (2014).
11. O. Reynolds, An experimental investigation of the circumstances which determine whether the motion of water shall be direct or sinuous, and of the law of resistance in parallel channels. *Proc. R. Soc. Lond.* **35**, 84–99 (1883).
12. T. Mullin, Experimental studies of transition to turbulence in a pipe. *Annu. Rev. Fluid Mech.* **43**, 1–24 (2011).
13. B. Eckhardt, T. M. Schneider, B. Hof, J. Westerweel, Turbulence transition in pipe flow. *Annu. Rev. Fluid Mech.* **39**, 447–468 (2007).
14. D. Barkley, Theoretical perspective on the route to turbulence in a pipe. *J. Fluid Mech.* **803**, P1 (2016).
15. S. C. C. Bailey, M. Hultmark, J. Schumacher, V. Yakhot, A. J. Smits, Measurement of local dissipation scales in turbulent pipe flow. *Phys. Rev. Lett.* **103**, 014502 (2009).
16. I. J. Wygnanski, F. H. Champagne, On transition in a pipe. Part 1. The origin of puffs and slugs and the flow in a turbulent slug. *J. Fluid Mech.* **59**, 281–335 (1973).
17. I. Wygnanski, M. Sokolov, D. Friedman, On transition in a pipe. Part 2. The equilibrium puff. *J. Fluid Mech.* **69**, 283–304 (1975).
18. B. Song, D. Barkley, B. Hof, M. Avila, Speed and structure of turbulent fronts in pipe flow. *J. Fluid Mech.* **813**, 1045–1059 (2017).
19. A. P. Willis, The openpipeflow Navier–Stokes solver. *SoftwareX* **6**, 124–127 (2017).
20. R. T. Cerbus, C.-c. Liu, G. Gioia, P. Chakraborty, Laws of resistance in transitional pipe flows. *Phys. Rev. Lett.* **120**, 054502 (2018).
21. S. Corrsin, An experimental verification of local isotropy. *J. Aeronaut. Sci.* **16**, 757–758 (1949).
22. S. G. Saddoughi, S. V. Veeravalli, Local isotropy in turbulent boundary layers at high Reynolds number. *J. Fluid Mech.* **268**, 333–372 (1994).
23. B. J. Rosenberg, M. Hultmark, M. Vallikivi, S. C. C. Bailey, A. J. Smits, Turbulence spectra in smooth- and rough-wall pipe flow at extreme Reynolds numbers. *J. Fluid Mech.* **731**, 46–63 (2013).
24. G. I. Taylor, Statistical theory of turbulence. *Proc. R. Soc. Lond. A* **151**, 421–444 (1935).
25. K. R. Sreenivasan, On the scaling of the turbulence energy dissipation rate. *Phys. Fluids* **27**, 1048–1051 (1984).
26. M. Eckert, The troublesome birth of hydrodynamic stability theory: Sommerfeld and the turbulence problem. *Eur. Phys. J. H* **35**, 29–51 (2010).
27. M. Sano, K. Tamai, A universal transition to turbulence in channel flow. *Nat. Phys.* **12**, 249–253 (2016).
28. G. Lemoult, L. Shi, K. Avila, S. V. Jalikop, M. Avila, B. Hof, Directed percolation phase transition to sustained turbulence in Couette flow. *Nat. Phys.* **12**, 254–258 (2016).
29. H.-Y. Shih, T.-L. Hsieh, N. Goldenfeld, Ecological collapse and the emergence of travelling waves at the onset of shear turbulence. *Nat. Phys.* **12**, 245–248 (2016).
30. Y. Pomeau, Front motion, metastability and subcritical bifurcations in hydrodynamics. *Physica D* **23**, 3–11 (1986).
31. Y. Pomeau, The long and winding road. *Nat. Phys.* **12**, 198–199 (2016).
32. G. Gioia, F. Bombardelli, Scaling and similarity in rough channel flows. *Phys. Rev. Lett.* **88**, 014501 (2001).
33. G. Gioia, P. Chakraborty, Turbulent friction in rough pipes and the energy spectrum of the phenomenological theory. *Phys. Rev. Lett.* **96**, 044502 (2006).
34. J. M. J. den Toonder, F. T. M. Nieuwstadt, Reynolds number effects in a turbulent pipe flow for low to moderate Re. *Phys. Fluids* **9**, 3398–3409 (1997).
35. S. G. Huisman, D. P. M. van Gils, C. Sun, Applying laser Doppler anemometry inside a Taylor–Couette geometry using a ray-tracer to correct for curvature effects. *Eur. J. Mech. B Fluids* **36**, 115–119 (2012).
36. H. Tennekes, J. L. Lumley, *A First Course in Turbulence* (MIT Press, 1972).
37. D. Moxey, D. Barkley, Distinct large-scale turbulent-laminar states in transitional pipe flow. *Proc. Natl. Acad. Sci. U.S.A.* **107**, 8091–8096 (2010).
38. S. B. Pope, *Turbulent Flows* (Cambridge Univ. Press, 2001).
39. R. A. Antonia, J. Kim, L. W. B. Browne, Some characteristics of small-scale turbulence in a turbulent duct flow. *J. Fluid Mech.* **233**, 369–388 (1991).
40. H.-E. Albrecht, N. Damaschke, M. Borys, C. Tropea, *Laser Doppler and Phase Doppler Measurement Techniques* (Springer, 2013).
41. R. J. Adrian, C. S. Yao, Power spectra of fluid velocities measured by laser Doppler velocimetry. *Exp. Fluids* **5**, 17–28 (1986).
42. S. Corrsin, *Local Isotropy in Turbulent Shear Flow* (National Advisory Committee for Aeronautics, 1958).
43. J. L. Lumley, Similarity and the turbulent energy spectrum. *Phys. Fluids* **10**, 855–858 (1967).

Citation: R. T. Cerbus, C.-c. Liu, G. Gioia, P. Chakraborty, Small-scale universality in the spectral structure of transitional pipe flows. *Sci. Adv.* **6**, eaaw6256 (2020).